THE LAW OF SIMILITUDE FOR VISCOUS HYPERSONIC FLOWS AROUND BLUNTED SLENDER BODIES

(ZAKON PODOBIA DLIA GIPERZVUKOVYKH OBTEKANII TONKIKH PRITUPLENNYKH TEL VIAZKIM GAZOM)

PMM Vol.25, No.6, 1961, pp. 1050-1059

V.V. LUNIEV
(Moscow)

(Received August 3, 1961)

Chernyi [1] developed the laws of hypersonic similarity for flows of ideal (inviscid) gases around blunted slender bodies. In [2], similarity laws were established for hypersonic flows of viscous heat-conducting gases around sharp slender bodies. Analogous results for this case were obtained by Cheng [3], and Hayes and Probstein [4]. In the present paper, general similarity laws for laminar hypersonic flows around blunted slender two-dimensional ($\nu = 0$) and axisymmetric ($\nu = 1$) bodies of viscous heat-conducting gases are developed. The laws of [1-4] follow from the present laws as special limiting cases. One also obtains laws of similitude for flows in inviscid high-entropy layers and for boundary-layer flows with variable entropy at the outer edge of the layer.

1. The characteristic feature of hypersonic flows around slender bodies in viscous heat-conducting gases is the separation of the disturbed field into two regions in which the governing parameters differ by an order of magnitude. The first region consists of the neighborhood of the strong oblique shock wave; there the temperature of the gas, which is weakly deflected, remains low in comparison with the stagnation temperature.

The second region comprises the high-temperature, or high-entropy, low-density layers brought about either by viscous dissipation or by compression through a (nearly) normal detached shock wave ahead of the blunted nose, or by both mechanisms.

At high Reynolds numbers $R_l = \rho_\infty U l/\mu_\infty$, where ρ_∞, μ_∞, U represent the density, viscosity and velocity of the free stream, and l the characteristic length of the slender body, the inviscid high-entropy region arises first. The usual boundary-layer, brought about by the no-slip

condition, develops at first within the high-entropy layer, gradually fills it and emerges from it only some distance from the nose. This distance decreases as the Reynolds number R_d (based on the diameter d of the section where blunting stops) decreases. When R_d decreases further (and the Mach number M of the free stream increases) the flow between the blunted nose and the detached shock wave becomes fully viscous [5], and the high-entropy layer is viscous throughout. Furthermore, for low R_d values, viscosity and heat conductivity can influence the motion of the gas in the high-entropy layer, which has acquired large vorticity in the passage through the curved strong shock, quite apart from the no-slip condition [6]. Under these conditions, the distinction between the essentially viscous region induced by the no-slip requirement at the wall, and the rest of the high-entropy layer becomes impossible. However, high-entropy layers possess many general properties, which allow a common approach to the problem.

Let xl and rl represent coordinates along and across the axis of the body, with the origin at its nose; uU and vU, velocity components in this coordinate system; $\rho_\infty U^2 p$ and $U^2 i$, the pressure and the specific enthalpy; a, the inclination of the shock wave; and β, the relative thickness of the body. Then, obviously, we shall have $u \sim 1$, $p \sim a^2$, $v \sim a$, $r \sim a$, and $x \sim 1$ inside the complete disturbed flow region, and $u \sim 1$ and $i \sim a^2$ in the shock layer. We note that in high-entropy layers with high temperatures we may have* $(1 - u) \sim u$ and the proposition $u \sim 1$ will not hold [7].

Henceforth, let us assume that the equation of state of the gas, the variation of viscosity $\mu_\infty \mu$ and of Prandtl number σ in the high-entropy regions have the form

$$\frac{p}{p_0} = \frac{\rho}{\rho_0} f_1(i), \quad \frac{\mu}{\mu_0} = C f_2(i), \quad \sigma = \sigma(i) \quad \left(C = \text{const} \sim 1,\ f_1 \sim \frac{i}{i_0}, i_0 \approx \frac{1}{2}\right) \tag{1.1}$$

Here the subscript 0 indicates stagnation conditions downstream of a normal shock. We obtain estimates for the pressure rise across the high-entropy layer from the r-component of the momentum equation and for the ratio λ between the flux across the high-entropy layer and the flux across the full disturbed region from the continuity equation:

$$\frac{\Delta p}{p} \sim \frac{\alpha\delta}{l} \frac{\rho}{p} \sim \frac{\rho_0}{p_0} \frac{\alpha\delta}{l} \frac{i_0}{i}, \qquad \lambda \sim \rho \frac{\delta}{\alpha l} \left(\frac{\beta l + \delta}{\alpha l}\right)^\nu \tag{1.2}$$

Here δ stands for the thickness of the high-entropy layer. In viscous high-entropy layers the enthalpy is on the order of stagnation enthalpy

---

* *Translator's Note.* See second paragraph in Section 3: *Added in proof.*

even in presence of high cooling at the wall. In the inviscid case let us introduce an effective adiabatic exponent γ_0, useful for the assessment of magnitudes at high temperatures (γ_0 takes values from 1.1 to 1.3 for dissociated air). Then in the special cases of the viscous and of the inviscid high-entropy layers we obtain*, respectively

$$i \sim i_0, \quad \rho \sim \rho_0 a^2; \qquad i \sim i_0 \left(\frac{p}{p_0}\right)^{(\gamma_0-1)/\gamma_0}, \quad \rho \sim \rho_0 a^{2/\gamma_0} \tag{1.3}$$

From the first equation (1.2) and from (1.3), it follows that for $a \ll 1$ the pressure may be considered constant across the high-entropy layer with an accuracy no less than $\rho_0 a^{2/\gamma_0}$. From the second equation (1.2), when $a \ll 1$, we have $\lambda \ll 1$, and consequently $a \sim M^{-1} + \beta + \delta/l$. Therefore, most of the mass of the disturbed gas passes outside of the high entropy layer. It is clear that a is small when the magnitudes M^{-1}, β and δ/l are small.

The order of magnitude of the thickness of the fully viscous high-entropy layer is estimated by standard boundary-layer methods. This thickness has a maximal order of magnitude when $a \sim \delta/l$. In such a case

$$\frac{\delta}{l} \sim \frac{1}{\alpha}\left(\frac{\mu_0}{\rho_0 R_l}\right)^{1/2} \sim \left(\frac{\mu_0}{\rho_0 R_l}\right)^{1/4} \tag{1.4}$$

The thickness of the fully inviscid high-entropy layer is determined by the constancy of mass flux across it. This flux has the order of magnitude $\pi^{\nu}\rho_{\infty} U d^{(1+\nu)}$, so that we have, for the same case, $a \sim \delta/l$

$$\frac{\delta}{l} \sim \frac{\alpha^{-2/\gamma_0} d^{1+\nu}}{\rho_0 l\,(l\beta+\delta)^{\nu}} \sim \rho_0^{-m}\left(\frac{d}{l}\right)^{m_0(1+\nu)}, \qquad m_0 = \gamma_0\,[2+\gamma_0(1+\nu)]^{-1}$$

Hence, for M^{-1} and β small, the order of a will be small if

$$\left(\frac{\mu_0}{\rho_0 R_l}\right)^{\frac{1}{4}} \ll 1, \qquad \left(\frac{d}{l}\right)^{m_0(1+\nu)} \ll 1 \tag{1.6}$$

2. Let us assume that the adiabatic exponent γ of the gas in the shock layer is the same as in the undisturbed free stream. Let us introduce the quantities

$$P = \frac{p}{\alpha^2}, \quad V = \frac{v}{\alpha}, \quad y = \frac{r}{\alpha}, \quad y_0 = \frac{r_0}{\alpha}$$

Here $r_0 = r_0(x)$ is the equation of the shock surface. Then the equations of motion in the shock layer and the various ratios across the

---

* In many cases the order of magnitudes in the high-entropy layer is the same for the viscous and inviscid cases; the smallness of $(\gamma_0 - 1)$ allows the assessment $a^{2(\gamma_0-1)/\gamma_0} \sim 1$, unless a is infinitesimally small.

shock take on the respective forms

$$\frac{\partial V}{\partial x}+V\frac{\partial V}{\partial y}=-\frac{1}{\rho}\frac{\partial P}{\partial y},\quad \frac{\partial}{\partial x}(\rho y^{\nu})+\frac{\partial}{\partial y}(\rho y^{\nu}V)=0,\quad \frac{\partial}{\partial x}\frac{P}{\rho^{\gamma}}+V\frac{\partial}{\partial y}\frac{P}{\rho^{\gamma}}=0 \tag{2.1}$$

$$P=\frac{1}{\gamma\theta_{\alpha}{}^{2}}+y_{0}'{}^{2}\left(1-\frac{1}{\rho}\right),\qquad V=y_{0}'\left(1-\frac{1}{\rho}\right)$$

$$\frac{1}{\rho}=\frac{\gamma-1}{\gamma+1}+\frac{2}{\gamma+1}\frac{1}{y_{0}'{}^{2}\theta_{\alpha}{}^{2}}\qquad(\theta_{\alpha}=M\alpha) \tag{2.2}$$

The general case of motion of the gas in the high-entropy region calls for the usage of the Navier-Stokes equations. Should the role of viscosity turn out to be unessential, the viscous terms will automatically cancel in the equations. However, for small α, with accuracy up to α^{2}, a group of the viscous terms in these equations can be neglected in the usual manner. With the pressure across the high-entropy layer constant, the equations of motion in this layer can then be reduced to the customary boundary-layer equations:

$$y^{\nu}\frac{P}{f_{1}}\left(u\frac{\partial u}{\partial x}+V\frac{\partial u}{\partial y}\right)=-ky^{\nu}\frac{dP}{dx}+N\frac{\partial}{\partial y}\left(y^{\nu}f_{2}\frac{\partial u}{\partial y}\right)$$

$$\frac{\partial}{\partial x}\left(\frac{P}{f_{1}}y^{\nu}u\right)+\frac{\partial}{\partial y}\left(\frac{P}{f_{1}}y^{\nu}V\right)=0 \tag{2.3}$$

$$y^{\nu}\frac{P}{f_{1}}\left(u\frac{\partial i}{\partial x}+V\frac{\partial i}{\partial y}\right)=ky^{\nu}u\frac{dP}{dx}+N\frac{\partial}{\partial y}\left(y^{\nu}\frac{f_{2}}{\sigma}\frac{\partial i}{\partial y}\right)+Ny^{\nu}f_{2}\left(\frac{\partial u}{\partial y}\right)^{2}$$

$$\left(k=\frac{p_{0}}{\rho_{0}},\quad N=\frac{k\chi^{2}}{\theta_{\alpha}{}^{4}},\quad \chi=\frac{M^{2}\mu_{0}{}^{1/2}}{(R_{l}/C)^{1/2}}\right)$$

At the body we impose the requirements

$$u=V=0,\qquad i=i_{w}(x)\quad\text{or}\quad\frac{\partial i}{\partial y}=q(x) \tag{2.4}$$

Since in the disturbed regions $y\sim 1$ it is permissible to drop the last term in the equation for the solid boundary $r=\beta r_{w}(x)+d/2l$, when at sufficiently large distance from the nose, and to satisfy the conditions (2.4) on the surface

$$r=\beta r_{w}(x)\ (r(0)=0)\quad\text{for}\quad d\ll 2\alpha l \tag{2.5}$$

In the shock layer $i\sim\alpha^{2}$, but according to (1.3) simultaneously $i\gtrsim i_{0}\,\alpha^{2(\gamma_{0}-1)/\gamma_{0}}$ in the high-entropy layer. Therefore at the edge of the high-entropy layer, $r=r_{\delta}(x)$, one can take, as in [2]

$$u\approx 1,\qquad i\approx 0,\qquad V_{+}=V_{-}\quad\text{for}\quad y=y_{\delta}=\frac{r_{\delta}}{\alpha} \tag{2.6}$$

Here V_{+} and V_{-} represent the limiting values of the function V as the edge $y_{\delta}(x)$ of the high-entropy layer is approached from within and from

without, respectively.

In the case of the fully viscous high-entropy layer its boundary with the shock layer is rather well defined [2,4]. In the inviscid case this boundary requires a somewhat more arbitrary definition; it can be identified with a streamline issuing from an arbitrary point of the transition section of the shock wave, which divides the regions with $a \sim 1$ from those with $a \ll 1$. Clearly, this transition section cannot extend far and is limited to the neighborhood of the blunted nose so that for bodies with $d/l \ll 1$ it can be assumed that the separation of the shock wave from the high-entropy layer takes place at the initial station $x \approx 0$. The whole disturbed region near $x \approx 0$ should be identified with the high-entropy layer, even though conditions $\delta \ll l$ and $\lambda \ll 1$ will not be satisfied here and Equations (2.3) may not be applicable.

3. In taking account of the small but finite blunt nose, we shall follow Chernyi [1] in the supposition that adequate solutions can be obtained by satisfying the conservation laws near $x \approx 0$ in their integral formulation and that the influence of the specific initial geometry on the important features of the flow damps out some distance from the nose. The parameters characterizing the role of the init factors are then to be determined from the integral form of the equations. For the high-entropy layer these equations read

$$\delta_1^{**} = \frac{1}{2}K_\alpha + \int_{y_w}^{y_\delta} Py^\nu dy - \int_0^x P\,(y_\delta^\nu y_\delta' - y_w\,y_w')\,dx + \frac{N}{k}\int_0^x \left(y_\nu f_2 \frac{\partial u}{\partial y}\right)_{y=y_w} dx$$

$$\vartheta_1 = L_\alpha + \frac{N}{k}\int_0^x \left(y^\nu \frac{f_2}{\sigma}\frac{\partial i}{\partial y}\right)_{y=y_w} dx$$

$$\delta_1^{**} = \frac{(\delta^{**})^{1+\nu}}{\alpha^{3+\nu}}, \qquad \vartheta_1 = \frac{\vartheta^{1+\nu}}{\alpha^{3+\nu}}, \qquad y_w = \frac{\beta}{\alpha}r_w, \qquad i_* = i + \frac{u^2}{2} + \frac{v^2}{2} \tag{3.1}$$

$$(\delta^{**})^{1+\nu} = \int_{r_w}^{r_\delta} \rho u r^\nu (1-u)\,dr, \qquad \vartheta^{1+\nu} = \int_{r_w}^{r_\delta} \rho u r^\nu (i_0 - i_*)\,dr$$

Here δ^{**} and $l\,\vartheta$ represent the momentum and the stagnation-enthalpy thickness of the boundary-layer theory. In the derivation of the first equation (3.1) we neglected a small quantity (of order a^2) corresponding to the momentum lost in the shock layer of the gas which enters the high-entropy layer. The constants K_α and L_α are determined from conservation of momentum and energy in the region D, which is bounded by the station $x \approx 0$ and by the front part of the shock wave. They are expressible in the form

$$K_\alpha = \frac{1}{2^\nu} C_x \alpha^{-(3+\nu)} \left(\frac{d}{2l}\right)^{1+\nu}, \qquad L_\alpha = \frac{1}{2^\nu} C_q \alpha^{-(3+\nu)} \left(\frac{d}{2l}\right)^{1+\nu}$$
$$C_x = c_x + c_\tau, \qquad C_q = \frac{Q\,(2/d)^{1+\nu}}{\pi^\nu \rho_\infty U^3} \tag{3.2}$$

Here C_x, c_x and c_τ stand for the coefficients of the complete drag, the wave drag and the friction drag of the nose, respectively. Q is the amount of heat lost by the gas per unit time in the region D, and C_q the mean Stanton number for the nose. In the preceding we neglected the pressure in the free stream in comparison with the pressure over the nose.

Let δ_0 and $u_0 U$ designate the viscous boundary-layer thickness over the blunted region and a characteristic gas speed at its outer edge, respectively, and ϑ a characteristic angle between the free-stream direction and the blunted surface. Then with $\sigma \sim 1$ we shall obtain

$$\frac{\delta_0}{d} \sim R_0^{-\frac{1}{2}} = \left(\frac{\mu_0}{\rho_0 u_0 R_d}\right)^{\frac{1}{2}}, \qquad c_\tau \sim u_0\, C_q \cos\vartheta, \quad C_q \sim \frac{\rho_0 u_0}{R_0^{1/2}} = \frac{\rho_0 u_0 \Delta}{d}\frac{\delta_0}{\Delta} \tag{3.3}$$

Should all the flow between the blunted surface and the shock wave be viscous, i.e. $\delta_0 \sim \Delta$, then $u_0 U$ would correspond to the tangential component of the velocity behind the shock wave at a point which is on the order of $d/2$ away from the axis. The quantity Δ has then the same order of magnitude as in the inviscid case* [5]. In agreement with Serbin [8], for $\rho_0 \gg 1$ we shall then have**, depending on the magnitude of ϑ

$$u_0 \sim 1, \quad \rho_0 \Delta \sim 1, \quad (\mu_0 / R_d)^{1/2} \sim k^{1/2} \quad \text{for } \cos\vartheta \sim 1$$
$$u_0 \sim k^{1/2}, \quad \Delta \sim k^{1/2}, \quad (\mu_0 / R_d)^{1/2} \sim k^{1/4} \quad \text{for } \cos\vartheta \ll 1 \tag{3.4}$$

In such a case then $C_q \sim 1$, and when $\cos\vartheta \sim 1$, the quantity $c_\tau \sim 1$, i.e. the viscous drag of the nose can be of the same order as the wave drag when $\delta_0 \sim \Delta$.

The relative contributions of the blunted and lateral surfaces to heat transfer and frictional drag can be characterized by the parameters ω_q and ω_τ, which according to (1.4) and (3.3) have the order

---

* At least as long as the thickness of the shock itself remains negligibly small in comparison with Δ.

** The case $\cos\vartheta \sim 1$ corresponds to sphere-like bodies and the case $\cos\vartheta \ll 1$ to disk-like bodies with the flattened face perpendicular to free-stream direction.

$$\omega_q \sim \frac{u_0^{1/2}}{\alpha}\left(\frac{d}{l}\right)^{1/2}\left(1+\frac{\beta l}{\alpha}\right)^{-\nu}, \qquad \omega_\tau \sim u_0\,\omega_q \cos\vartheta \tag{3.5}$$

The relative contributions to the drag due to the blunted nose and due to friction over the lateral surfaces are characterized by the parameter

$$\omega_0 \sim C_x\left(\frac{R_l}{\mu_0\rho_0}\right)^{1/2}\frac{d}{\alpha l}\left(1+\frac{\beta l}{d}\right)^{-\nu}$$

The motion of the gas in the high-entropy region is fully described by Equations (2.3) or (3.1) so that the momentum balance in the direction normal to the body axis appears unessential. The ratio between the momenta normal to the axis integrated over the high-energy layer and over the shock layer, respectively, is of the same order as the ratio of the corresponding fluxes, $\lambda \ll 1$. Consequently, if the impulse in that direction imparted to the gas by the blunted region* (designated by $I(1/2\ d)^{1+\nu}\rho_\infty U$ per unit width in a direction normal to the free-stream direction, or per unit angle between meridional planes in the axisymmetric case) has an influence on the motion in the large, then this impulse must enter into the corresponding integral equation for the shock layer, namely

$$\int_{y_\delta}^{y_0}\rho V y^\nu dy = J_\alpha + \int_0^x\left[P(y_\delta)\,y_\delta^\nu + \int_{y_\delta}^{y_0} P dy\right]dx \qquad \left(J_\alpha = \frac{I}{\alpha^{2+\nu}}\left(\frac{d}{2l}\right)^{1+\nu}\right) \tag{3.6}$$

The parameters K_α and J_α are analogous to those used by Chernyi [1].

In this manner, the influence of viscosity does not introduce new (relative to the inviscid case) parameters characterizing the blunting. The heat transfer between the nose surface and the stream brings about a new determining parameter L_α. When the nose is insulated L_α reduces to zero, if in the region D other sources or sinks of energy are absent (radiation from the gas cap, transpiration cooling, etc.).

4. The derived equations and the boundary conditions contain the parameters

$$\gamma,\ \theta_\alpha,\ \chi,\ k,\ K_\alpha,\ L_\alpha,\ J_\alpha \tag{4.1}$$

The parameter β/α is determined in the process of solution and appears as a function of parameters (4.1), which can therefore be reduced to

---

* *Translator's Note.* See pp. 205 and 219 of English edition of [1].

$$\gamma,\ \theta,\ \chi,\ k,\ K,\ L,\ J \tag{4.2}$$

$$\left(\theta = M\beta,\ K = \frac{1}{2^{\nu}}\frac{C_x}{\beta^{3+\nu}}\left(\frac{d}{2l}\right)^{1+\nu},\ L = \frac{1}{2^{\nu}}\frac{C_q}{\beta^{3+\nu}}\left(\frac{d}{2l}\right)^{1+\nu},\ J = \frac{I}{\beta^{2+\nu}}\left(\frac{d}{2l}\right)^{1+\nu}\right)$$

Under the stipulated assumptions, the parameters (4.2) form the complete system of similarity parameters for hypersonic flows of a viscous heat-conducting gas around bodies which have the same shape $r_w(x)$, obey the same heat-transfer conditions (2.4), but are blunted in different manner.

For bodies with negligibly small blunting, i.e. for $K_\alpha \approx L_\alpha \approx J_\alpha \approx 0$, the parameters K, L and J fall out of the system (4.2). In that case, the conditions of similitude (4.2) differ from those of [2] only because of the more general specification of the gas (1.1), which leads to a modification of the parameter χ and to the appearance of the new parameter k (whereas in [2], $k = k(\gamma)$).

The system (4.1) contains three parameters K_α, L_α and J_α, or the equivalent group K_α, Ia/C_x and C_q/C_x, which characterize the influence of the nose blunting. The quantities c_x and I depend on the parameter k and on the form of the blunting, while c_τ and C_q depend also on the parameter $(\mu_0/R_d)^{1/2}$. One can therefore conclude that when the first five parameters (4.1) or (4.2) are kept constant, there are essentially no degrees of freedom left, except for the form of the blunting, with which to satisfy the remaining criteria of similitude, Ia/C_x = const and C_q/C_x = const.

However, if the class of admissible cases is restricted by the requirement

$$K_\alpha \lesssim \alpha^{-m} \qquad (m > 0) \tag{4.3}$$

and in the viscous axisymmetric problem by the requirement $a^n \sim \beta \gtrsim d/l$, then, with $C_x \sim 1$, we shall have*

$$J_\alpha \sim \alpha^{1-m} \ll 1,\quad \omega_q \lesssim \alpha^{m_1+\nu(1-n)} \ll 1 \quad \text{for} \quad m < 1,\quad \frac{8-3m}{4} > n \geqslant 1$$

$$\left(m_1 = \frac{1-m+(3-2m)\nu}{2(1+\nu)}\right)$$

---

* The condition (4.3), $K_\alpha \lesssim \alpha^{-m}$, automatically leads to the inequality $d/al \lesssim \alpha^{(2-m)/(1+\nu)} \ll 1$, so that, generally speaking, (4.3) represents a more stringent constraint on the realm of applicability of the similitude than the earlier adopted condition $d \ll al$.

Therefore, J and L can be excluded from the system of similarity criteria (4.2). We note that the remaining parameters essentially do not contain any which were not introduced in the earlier studies [1,2] of special limiting cases of the law of similitude.

From general expressions for the heat-transfer coefficient and for the friction coefficient it follows easily that when the similarity conditions are satisfied, the quantities c_q/a^3 and c_f/a^3 remain invariant. Here c_q and c_f designate local heat flux and local surface shear nondimensionalized with $\rho_\infty U^3$ and $\rho_\infty U^3$, respectively.

5. The scheme of satisfying equations and boundary conditions in the nose region of a viscous high-entropy layer in an integrated form can be justified on the basis of the general behavior of viscous and heat-conducting flows. Viscosity and heat-conduction smooth out differences incurred in the initial distribution of the parameters in the high-entropy layer so that some distance downstream the decisive role will be played by the integrated characteristics of the initial conditions. At high Reynolds numbers, when the high-entropy layer is partly nonviscous, the differential distribution of entropy across its streamlines is preserved outside the boundary layer for longer distances from the nose (until the boundary layer fills the high-entropy layer entirely). Also, the conditions $i \approx 0$ and $u \approx 1$ are no longer satisfied at the edge of the boundary layer. In fact, the characteristics of the boundary layer depend on the distribution of entropy along its outer edge.

In this connection, let us examine more closely the similarity conditions for the distribution of parameters in a partly or fully inviscid high-entropy layer. Ultimately, for cases of similitude, we expect coincidence of the profiles $i(x, y)$ and $u(x, y)$. In the boundary layer, the influence of conditions near $x \approx 0$ can clearly be disregarded. Then it follows from (2.3) that similitude in the boundary layer takes place when the same functions $i = i_1(x)$ and $u = u_1(x)$ are prescribed at its outside edge $y = y_1(x)$. In the inviscid region, where the flow is isentropic, the functions $i(x, y)$ and $u = (1 - 2i)^{1/2}$ will be identical for the cases of similitude if the entropy and pressure fields $s(x, y)$ and $p(x, y)$ are the same, respectively. In general, the coincidence of the pressure fields $p(x, y)$ will not occur, but that can be disregarded because of the weak dependence of enthalpy on pressure. In fact, we have conditions

$$i \approx {}^1/_2\, p^{(\gamma_0-1)/\gamma_0}(\sin \varepsilon)^{2/\gamma_0}$$

where ϵ is the angle of the shock wave at the point of intersection with a given streamline. Since the difference $\gamma_0 - 1$ is small, especially for high-temperature air, the function i depends on p very weakly and for

$\gamma_0 \to 1$ becomes altogether independent. Thus, if we accept the condition $\gamma_0 - 1 \ll 1$ as an additional constraint, we can assert that the enthalpy and the velocity in the high-entropy layer depend only on the entropy*. Henceforth, we shall take $s = \sin^2 \epsilon$.

Let $\psi\rho_\infty U(1/2\ d)^{1+\nu}$ designate the mass flux between the body and the given point of interest. Then

$$\varphi = \frac{\psi}{C_x} = \frac{P}{kK}\int_{y_w}^{y} \frac{u}{f_1(i)} y^\nu dy \quad (5.1)$$

$$y^{1+\nu} - y_w^{1+\nu} = \frac{2^\nu kK}{P}\int_0^\varphi \frac{f_1(i)}{u}\, d\varphi$$

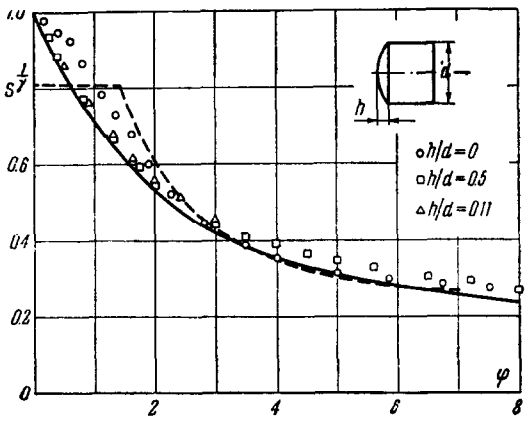

Fig. 1.

If, for fixed values of the similitude parameters, the functions $u(x, y)$ and $i(x, y)$ should be universal functions of its variables, then $x(x, y)$ and, according to (5.1), $\phi(x, y)$ would also be universal function. However, for different nose shapes, the functions $s(\psi) = s(C_x\phi)$ will generally be different. Hence, if $s(x, y)$ and $\phi(x, y)$ in the inviscid part of the high-entropy layer are to be universal, then we must require that for the cases of similitude, the functions $s(\phi)$ be identical.

Conversely, if for cases of similitude in the inviscid part of a high-entropy layer the functions $s(\phi)$ are identical (and consequently also the functions $i(\phi)$ and $u(\phi)$, then clearly the functions $i(x, \phi)$ and $u(x, \phi)$ in the boundary layers will be identical and so will be the edges** of the boundary layers $\phi = \phi_1(x)$. Consequently, in accordance with (5.1), the functions $i(x, y)$ and $u(x, y)$ in the high-entropy layer will be universal functions of its variables for all the cases of

---

* More exactly, we should require $(a_1/a_2)^{2(\gamma_0-1)/\gamma_0} \approx 1$ if there is to be similitude in the high-entropy layer for different cases $a = a_1$ and $a = a_2$. The condition $\gamma_0 - 1 \ll 1$ will not be necessary for $a_1 = a_2$ (for instance for flows around identical bodies which differ only in nose shape).

** This edge is determined from the condition of smoothness of the profiles i and u.

similitude.

In this manner, the developed law of similitude remains valid in the complete disturbed region of flow (with the possible exception of a very thin region between the high-entropy layer and the shock layer) if $\gamma_0 - 1 \ll 1$ and the function $s(\phi)$ is identical for the cases of similitude.

For high Reynolds numbers the quantity C_x and the shape of the shock wave depend only on the parameter k, because when the blunted shape is invariant the functions $s(\phi)$ will be identical for the cases of similitude. We can suppose that for equal values of k, the functions $s(\phi)$ for different blunted noses (in the vicinity of the detached shock wave of for $\phi \gtrsim 1$) will not materially differ among themselves. Justification for the supposition can be found in Fig. 1, which displays the values of $[s(\phi)]^{1/\gamma}$ for different blunt bodies at $M = 6$, $\gamma = 1.4$. The experimental values were collected from different sources while the theoretical values correspond to a sphere (solid line) and to a cone-cylinder (half-angle of 50°-dotted line). It can be seen that the functional values are sufficiently close to each other in spite of the large differences in the shapes of the bodies. This universal character of the function $s(\phi)$ should be, of course, verified for smaller values of k before undertaking further deductions concerning the limits of applicability of the laws of similitude*.

We can expect that any differences between the functions $s(\phi)$ and any dependence of i on the pressure will not particularly influence the similitude of the essential features of the boundary layer (c_q, c_f, displacement thickness δ^*). Of this we may easily be convinced if we make the assumption that such features depend only on local conditions, which is fully acceptable for qualitative deductions. Setting $f_1 = f_2$ and, for the evaluation of δ^*, $\rho\mu = \text{const}$, and $\sigma = 1$, we have

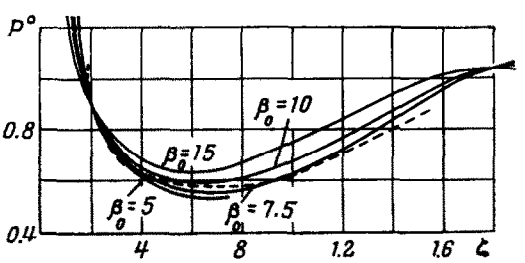

Fig. 2.

* For $k \to 0$, the front part of the shock wave follows the shape of the body. However, the difference between the actual shape of the shock wave and this limiting shape disappears only as $k^{1/2}$ (especially for bodies with $\cos\phi \ll 1$) and can therefore be substantial for the regime $k \gtrsim 0.05$ of practical interest. Thus, it is rather likely that the function $s(\phi)$ will be nearly universal for these conditions as well as for $\phi \lesssim 1$.

$$\frac{c_q}{\alpha^3} = \frac{A_1 u_1^{1/2} x^{1/2} \chi}{(kP)^{1/2} \Theta_\alpha^2} \qquad \frac{c_f}{\alpha^3} = \frac{A_2 x^{1/2} u_1^{3/2} \chi}{(kP)^{1/2} \Theta_\alpha^2}$$
$$\frac{\delta^*}{\alpha l} = A_3 x^{1/2} (i_1 + 0.78 - 0.65 i_w) \chi \frac{k^{1/2} P^{-1/2}}{\Theta_\alpha^2 u_1^{1/2}} \tag{5.2}$$

Here A_1, A_2 and A_3 are coefficients*. It is easy to see that Expressions (5.2) depend relatively weakly on i_1 when i_1/i_0 is not too close to unity, so that differences in $s(\phi)$ and p indeed make little imprint on the features of the boundary layer. We note that the function i_1 decreases as γ_0 grows, and thus, according to (5.2), the similitude of the boundary-layer characteristics depends less and less on $(\gamma_0 - 1)$ and on the universality of the function $s(\phi)$.

As to the effect of differences in the functions $s(\phi)$ on the pressure distributions along the body in the inviscid high-entropy layer, it will be relatively small. In fact, Expression (5.1) for the thickness of the high-entropy layer contains the function $s(\phi)$ only under the integral sign, a fact which must reduce the net influence of the departures of $s(\phi)$ from the universal values.

We have ample reasons that because of the effects of viscosity and heat-conductivity, which smooth out the differences in the initial conditions at the nose, and apparently because of the increase in the thinness of the intermediate zone between the layers, the accuracy of the law of similitude will be greater in the case of the viscous high-entropy layer. In this connection, some idea of the accuracy of the law of similitude can be obtained from Fig. 2, which displays various pressure distributions, obtained by exact numerical computations for an inviscid gas with $\gamma = \gamma_0 = 1.4$ and $M = \infty$. The solid curves correspond to different spherically blunted cones of semiangles β_0 and the dotted curve to a cone of semiangle $\beta_0 = 10°$ blunted by another cone of semiangle $50°$. In these cases, there is not characteristic length l and the distributions $P^\circ(\zeta) = p/\beta_0^2$ for all cones should coincide as functions of the abscissa $\zeta = (2^3/C_x)^{1/2} \beta_0^2 l/d$, [1]. The exhibited curves are indeed sufficiently contiguous even though the magnitude of the pressures and of the domain of influence of the nose in the cases $\beta_0 = 5$ and $\beta_0 = 15°$ differ ninefold. Some of the differences between the curves for different β_0

---

* With the help of these coefficients we could account for the "prehistory" of the boundary layer, i.e. the distribution of the function $P(x)$ on the surface of the body, the shape of the body, etc.

can evidently be accounted for by the deviation from similitude in the high-entropy layer caused by the insufficient smallness of $(\gamma_0 - 1)$. Here the thickness δ of the high-entropy layer decreases more slowly as a grows then for $\gamma_0 = 1$, since $\delta \approx p^{-1/\gamma_0}$, which thus leads to an increase in $P^\circ(\zeta)$.

The author thanks V.G. Pavlov for his great help in computations.

Added in proof. Recently, [9] was published, where, for a perfect gas, σ = const, and $\mu \sim i^n$, essentially the same similarity criteria were obtained as in Section 4. One difference is that instead of the parameters K, χ and θ, the authors used combinations thereof. Also, the parameters L and I were not introduced and the conditions under which they can be neglected were not investigated.

In order to avoid difficulties connected with the study of the flow in the high-entropy layer, and to reduce the derivation of the law of similitude to collation and synthesis of the previously known results [1-4], the authors of [9] assume that for an inviscid high-entropy layer $u \approx 1$. However, this condition is not satisfied in many cases (e.g. on the surface of a blunted wedge with $\beta = 10^\circ$ where the magnitude $u \approx 0.5$ to 0.8 for $\gamma_0 = 1.1$ to 1.4).

Furthermore, the condition $u \approx 1$ does not erase the dependence upon the entropy distribution of the thickness of the high-entropy layer and consequently of the magnitude of P and V in the whole disturbed region. (The exceptional case [9] of $\gamma = \gamma_0 \to 1$ is not consistent with the assumption $u \approx 1$, inasmuch as $u \to 0$ as $\gamma_0 \to 1$.)

In the present paper it is shown that compliance with the criteria of similitude, developed in Section 4 and in [9], is insufficient for similitude in the inviscid case, for which the universality of the entropy distribution $s(\phi)$ is mandatory. In the framework of the blast-wave analogy we have s = const ϕ^{-1} for flows around blunt cylinders or plates. Since this analogy is applicable only at large distances from the nose, the fact of the universality of the function $s(\phi)$ in the neighborhood of the nose (Fig. 1) appears altogether remarkable.

BIBLIOGRAPHY

1. Chernyi, G.G., *Techenie gaza s bol'shoi sverkhzvukovoi skorostiu.* Fizmatgiz, 1950. (English translation by R. Probstein: *Introduction to Hypersonic Flows,* Academic Press, 1961.)

2. Luniev, V.V., O podobii pri obtekanii tonkikh tel viazkim gazom pri bol'skikh sverkhzvukovykh skorostiakh (On the similarity of viscous hypersonic flows around slender bodies). *PMM* Vol. 23, No. 1, 1959.

3. Cheng, H., Similitude of hypersonic real-gas flows over slender bodies with blunted noses. *JAS* No. 9, 1959.

4. Hayes, W. and Probstein, R., Viscous hypersonic similitude, *JAS* No. 12, 1959.

5. Adams, M. and Probstein, R., On the validity of continuum theory for satellite and hypersonic flight problems at high altitude. *Jet Propulsion* No. 2, 1958.

6. Ferri, A., Vliianie krivizny udarnoi volny na povedenie giperzvukovogo pogranichnogo sloia (The effect of shock-wave curvature on the behavior of hypersonic boundary layers). Report of the All-Soviet Congress on Theo. and Appl. Mech., Moscow, 1960. Coll. foreign translations, *Mekhanika* No. 5, 1960.

7. Luniev, V.V., O dvizhenii v atmosfere zatuplennogo tela s bol'shimi sverkhzvukovymi skorostiami (On the flight of hypersonic blunted bodies). *Izv. Akad. Nauk, SSSR, OTN, Mekh. i Mash.* No. 4, 1959.

8. Serbin, H., The high-speed flow of gas around blunt bodies. *Aeronautical Quarterly* Vol. 9, No. 4, 1958.

9. Cheng, H. *et al.*, Boundary-layer displacement and leading-edge bluntness effects in high-temperature hypersonic flow. *JAS* No. 5, 1961.

Translated by M.V.M.